Trans. Phenom. Nano Micro Scales, 7(2): 97-112, Summer and Autumn 2019
DOI: 10.22111/tpnms.2019.27933.1164

**ORIGINAL RESEARCH PAPER**

# Numerical study of fins arrangement and nanofluids effects on three-dimensional natural convection in the cubical enclosure

***Mohammad Mohsen Peiravi[1], Javad Alinejad[2,*], Davood Domairry Ganji[3], Soroush Maddah[4]***

*[1,2,4]Department of Mechanical Engineering, Sari Branch, Islamic Azad University, Sari, Iran*
*[3]Department of Mechanical Engineering, Noshirvani-Babol University, Babol, Iran*

*Received 10 December 2018; revised 18 January 2019; accepted 2 February 2019; available online 29 July 2019*

**ABSTRACT:** This investigation is a three dimensional comprehensive heat transfer analysis for partially differentially heated enclosure with the vertical fin mounted on the hot wall. The thermal lattice Boltzmann based on D3Q19 method is utilized to illustrate the effects of vertical fins and nanoparticles on the flow and thermal fields. The effects of Rayleigh number and different arrangement of fins on the fluid flow and heat transfer have been scrutinized. The streamlines and isotherms and Nusselt number along the hot wall are illustrated for $10^4<Ra<10^8$ and nanoparticles volume fraction $0.01<\varphi<0.03$. The results signified that by choosing the suitable arrangement for the fins (three fins in $Ra=10^6$ and two fins in $Ra=10^4$), the average Nu could be increased by more than 60%, but the effect of using the nanofluids ($\varphi$=0.03, Cuo/Water) is less than 30%. So arrangement of fins and nanofluids ($\varphi$=0.03, Cuo/Water) effects improve the heat transfer mechanism in the cubical enclosure.

**KEYWORDS:** *Cubical enclosure; Lattice Boltzmann method; nanoparticles effects; natural convection; vertical fins*

## INTRODUCTION

Three-dimensional natural convection heat transfers in differentially heated cubical cavity with vertical fins attached to their active walls has many industrial applications including energy storage systems, thermal control of electronic devices, cooling of radioactive waste containers, and ventilation of rooms, to name a few. In these applications, vertical rectangular parallelepiped fins are widely used to augment heat transfer because of their simplicity and lower cost, so it motivated the researchers to improve their accuracy by different ways such as experimentally, numerically or analytically.

Not only fins improve the heat transfer mechanism, but also nanofluids can assist the heat transfer in industries which both of these two ways are considered in this literature review. Above-mentioned industrial applications of the natural convection heat transfer are associated with 3D phenomena. However, less effort in the literature has been devoted to the 3D numerical simulation of those problems [1]. In an attempt to solve many problems, particularly in fluid mechanics, the Lattice Boltzmann method (LBM) [2-3] has been evolving over the last two decades. Physics of microscopic processes are taken into account by simplifying kinetic models in LMB. Fluid flows are then anticipated through the evolution of one-particle phase space distribution functions on associated macroscopic average properties. LBM simulations, based on the gas kinetic theorem, are based on two simple steps:

Particle distribution "collision" on Lattice nodes and stream "propagation" from one node to all neighbors along the Lattice directions.

Once streaming is done new distribution components of Lattice nodes are calculated, from which we obtain the updated macroscopic properties. This method of calculating macroscopic values essentially differs from what is done in other traditional CFD methods. Algorithm simplicity, fully parallel computation and easy implementation of complex boundary conditions are among the numerous superiorities of LBM [4-5]. The lattice Bhatnagar-Gross-Krook (LBGK) model which is the most popular LBM is known for its remarkable abilities to solve complex fluid flow problems such as natural convection flow, multiphase fluids and suspensions in fluids. Benzi et al. [6], examined the basic elements of the Lattice Boltzmann equation network theory, a special kinetic model of class gas for hydrodynamics and fluid flow. Ladd [7], performed hydrodynamics simulation using 32,000 solid particles and the Lattice Boltzmann method. Nestler et al. [8], studied combination of Lattice Boltzmann and phase-field simulations for incompressible fluid flow in porous media. Succi et al. [9], studied application of the lattice Boltzmann equation to multiscale physics in fluids. Prasianakis et al. [10], it has shown a strong potential in simulating nonlinear mathematical-physical equations [11-13]. It should be noted that these models always deal with stability issues and therefore in the last few years, several researches have been done to solve this problem [14-17] such as TRT models and multi-relaxation-time (MRT) model.

✉ *Corresponding Author Email: *alinejad_javad@iausari.ac.ir*
Tel.: +981133032891; Note. This manuscript was submitted on December 10, 2018; approved on January 18, 2019; published online July 29, 2019.

**Nomenclature**

| | |
|---|---|
| $A_{DL}$ | Ratio of the total surface of hot wall |
| $c_i$ | Lattice velocity |
| $c_s$ | Lattice speed |
| $c_p$ | Specific heat capacity |
| $d_f$ | Spherical particle diameter of the fluid |
| $d_s$ | Spherical particle diameter of the solid |
| $f_i$ | Particle density distribution function |
| $f_i^{eq}$ | Equilibrium particle density distribution function |
| F | External force |
| $g_i$ | Particle energy distribution function |
| $g_i^{eq}$ | Equilibrium particle energy distribution function |
| $g_y$ | Gravitational acceleration |
| $h_f$ | Fines height |
| H | Dimensions of the cubical enclosure |
| J | Joel |
| K | Kelvin |
| K | Thermal conductivity |
| kg | Kilogram |
| $k_f$ | Thermal conductivity of the fluid |
| $k_s$ | Thermal conductivity of the solid |
| $k_{nf}$ | Nanofluid thermal conductivity |
| $k_b$ | Boltzmann constant |
| $L_f$ | Fines length |
| $l_f$ | Mean path of the fluid particle |
| m | Meter |
| $Nu_m$ | Mean Nusselt number |
| $Nu_y$ | Local Nusselt number |
| $n_1, n_2$ | Relaxation time constants |
| Pr | Prandtel number |
| $q_{DL}$ | Rate of heat transfer with fin per heat transfer without fin |
| Ra | Rayleigh number |
| Re | Reynolds number |
| S | Distance between each of two fins |
| t | Time |
| T | Temperature |
| $T_h$ | Temperature of the hot wall |
| $T_c$ | Temperature of the cold wall |
| u, v, w | Velosities |
| $w_f$ | Fines width |
| $\omega_i$ | Lattice grade weight |
| W | Watt |
| x, y, z | Coordinates |

**Greek Letters**

| | |
|---|---|
| $\alpha$ | Thermal diffusivity |
| $\alpha_f$ | Thermal diffusivity of the fluid |
| $\alpha_{nf}$ | Nanofluid thermal diffusivity |
| $\beta$ | Thermal expansion coefficient |
| $\beta_f$ | Thermal expansion coefficient of the fluid |
| $\beta_s$ | Thermal expansion coefficient of the solid |
| $\beta_{nf}$ | Nanofluid Thermal expansion coefficient |
| $\theta$ | Dimensionless temperature |
| $\mu$ | Dynamic viscosity |
| $\mu_f$ | Dynamic viscosity of the fluid |
| $\mu_{nf}$ | Nanofluid dynamic viscosity |
| $\upsilon$ | Kinematic viscosity |
| $\rho$ | Density |
| $\rho_f$ | Density of the fluid |
| $\rho_s$ | Density of the solid |
| $\rho_{nf}$ | Nanofluid density |
| $\tau_v$ | Relaxation time relating to flow field |
| $\tau_c$ | Relaxation time relating to temperature field |
| $\phi$ | Nanofluid volume fraction |
| $\Delta T$ | Temperature difference |

**Subscript**

| | |
|---|---|
| c | Cold |
| DL | Dimension less |
| f | Fluid |
| h | Hot |
| i | Direction of lattice link |
| nf | Nanofluid |
| s | Solid |

## SIMULATION METHODOLOGY

### Lattice Boltzmann method

The thermal Lattice Boltzmann equations [22] based on a uniform Lattice with BGK collision model are as follows:

$$f_i(x + c_i\Delta t.\, t + \Delta t) - f_i(x.t) = -\frac{\Delta t}{\tau_v}\left(f_i(x.t) - f_i^{eq}(x.t)\right) + \Delta t c_i F_i \quad (1)$$

$$g_i(x + c_i\Delta t.\, t + \Delta t) - g_i(x.t) = -\frac{\Delta t}{\tau_c}\left(g_i(x.t) - g_i^{eq}(x.t)\right) \quad (2)$$

Where $c_i$ is the Lattice velocity, while $f_i$ and $g_i$ are the particle density and energy distribution functions, respectively. $\tau_v$ and $\tau_c$ are the controlling factors of the rate equilibrium. The equilibrium density distribution function and the equilibrium energy distribution for the current 3D application, based on D3Q19 model, are expressed as:

$$f_i^{eq} = \omega_i \rho \left[1 + \frac{c_i \cdot u}{c^2} + \frac{9(c_i \cdot u)^2}{2c^4} - \frac{3u^2}{2c^2}\right] \quad (3)$$

where $\omega_0 = \frac{1}{3}$, $\omega_i = \frac{1}{18}$ for i=1-6 and $\omega_i = \frac{1}{36}$ for i=7-18.

$$g_0^{eq} = -\frac{T}{2}\frac{u^2}{c^2},$$
$$g_{1-6}^{eq} = \frac{T}{18}\left[1 + \frac{c_i \cdot u}{c^2} + \frac{9(c_i \cdot u)^2}{2c^4} - \frac{3u^2}{2c^2}\right] \quad (4)$$
$$g_{7-18}^{eq} = \frac{T}{36}\left[2 + 4\frac{c_i \cdot u}{c^2} + \frac{9(c_i \cdot u)^2}{2c^4} - \frac{3u^2}{2c^2}\right]$$

As mentioned before, Navier-Stokes equations can be extracted in this model. By using Chapman-Enskog expansion the kinematic viscosity (υ) and the thermal diffusivity (α) are related to the relaxation times by:

$$\vartheta = [\tau_v - 1/2]c_s^2\Delta t \quad (5)$$

$$\alpha = [\tau_c - 1/2]c_s^2\Delta t \quad (6)$$

Where $c_s$ is the lattice speed of sound expressed as:

$$c_s = \frac{1}{\sqrt{3}}\frac{\Delta x}{\Delta t} \quad (7)$$

It should be noted that by choosing $\Delta x = \Delta t = 1$, it is possible to make the variables dimensionless. Finally, macroscopic variables $\rho$, $u$ and $T$ can be calculated using the following equations:

Flow density:

$$\rho(x.t) = \sum_{i=0}^{18} f_i(x.t) \quad (8)$$

Momentum:

$$\rho u(x.t) = \sum_{i=0}^{18} c_i f_i(x.t) \quad (9)$$

Temperature:

$$T(x.t) = \sum_{i=0}^{18} g_i(x.t) \quad (10)$$

Where F presents the acting external force per unit mass defined as:

$$F = \rho g_y \beta \Delta T \quad (11)$$

$g_y$ .β and ΔT are gravitational acceleration, thermal expansion coefficient and temperature difference, respectively.

For modeling the nanofluid because of changing in the fluid thermal conductivity, density, heat capacitance and thermal expansion, some of the governed equations should be changed.

Thermo-physical nanofluid properties except density, which is obtained by Boussinesq approximation, are assumed invariant, and are given in Table 1.

**Table 1**
Thermo-physical properties of water and nanoparticles.

| **Material** | **ρ (kg/m$^3$)** | **$C_P$ (J/kgK)** | **k (W/mK)** | **β×10$^5$ (k$^{-1}$)** |
|---|---|---|---|---|
| Pure water | 997.10 | 4179 | 0.61 | 21 |
| Copper (CuO) | 8954 | 383 | 400 | 1.67 |
| Alumina ($Al_2O_3$) | 3970 | 765 | 40 | 0.85 |

The thermal diffusivity is written as:

$$\alpha_{nf} = \frac{k_{nf}}{(\rho c_p)_{nf}} \quad (12)$$

The effect of density at reference temperature is given by:

$$\rho_{nf} = (1-\phi)\rho_f + \phi\rho_s \quad (13)$$

And the heat capacitance and thermal expansion of nanofluid can be given as [41]:

$$(\rho c_p)_{nf} = (1-\phi)(\rho c_p)_f + \phi(\rho c_p)_s \quad (14)$$

$$\beta_{nf} = (1-\phi)\beta_f + \phi\beta_s \quad (15)$$

The viscosity of the nanofluid containing a dilute suspension of small rigid spherical particles is given by the Brinkman model [42] as:

$$\mu_{nf} = \frac{\mu_f}{(1-\phi)^{2.5}} \quad (16)$$

The effective thermal conductivity of the two component entities of spherical-particle suspension was introduced by Chon et al. [43] as follows

$$\frac{k_{nf}}{k_f} = 1 + 64.7\,\phi^{0.764}\left(\frac{d_f}{d_s}\right)^{0.369}\left(\frac{k_f}{k_s}\right)^{0.7476} Pr_T Re_T^{1.2321} \quad (17)$$

Where $Pr_T$ and $Re_T$ are given as:

$$Pr_T = \frac{\mu_f}{\rho_f \alpha_f}. \quad Re_T = \frac{\rho_f k_b T}{3\pi\mu_f^2 l_f} \quad (18)$$

Where $l_f$ is the mean path of the fluid particle (17nm) and $k_b$ is the Boltzmann constant.

## Appropriate relaxation time for natural convection

Deducted from fundamental Lattice Boltzmann references [44-45], maximum convergence possibility for a specified grid can be reached with regard to the following two principals:

1. Maximum velocity should not exceed the critical velocity of 0.1.
2. Relaxation times in unsteady problems must be as large as possible.

We start with the first condition to find the suitable relaxation time:

In natural convection problems maximum velocity is not known in advance, so a scale analysis of the natural convection boundary layer as follows is necessary:

$$\text{For Pr} < 1: u_{max} \sim \frac{\nu}{H}\left(\frac{Ra}{Pr}\right)^{1/2} \tag{19}$$

$$\text{For Pr} > 1: u_{max} \sim \frac{\nu}{H}\left(\frac{Ra^{1/2}}{Pr}\right) \tag{20}$$

The right hand sides of the above proportionalities consist of two parts.

The former is arbitrary for the selected case and does not affect the final result, the latter depends on the physical characteristics of the problem, the Prandtel number and Rayleigh number defined by $\text{Pr} = \nu/\alpha$ and $\text{Ra} = g\beta(T_h - T_c)\text{H}^3\text{Pr}/\nu^2$, and is constant once the problem is specified.

Proportionalities 19 and 20 can be converted to equalities using constants $n_1$ and $n_2$. These constants could be calculated for different geometries by solving the problem in a more stable condition compared to the ones which deal with stability issues. For instance, by comparing the two sides of these inequalities, we obtained $n_1$=0.25 for a 2-D convective square cavity problem with Ra = $10^6$. The fact that $n_1$, and possibly $n_2$, is less than unity is an important result, which has not been mentioned in the previous works [46-47].

$$\text{For } \text{Pr} < 1: u_{max} = n_1 \frac{\nu}{H}\left(\frac{Ra}{Pr}\right)^{\frac{1}{2}} \rightarrow \nu = \frac{u_{max}}{n_1}\left(\frac{Pr}{Ra}\right)^{1/2} H \tag{21}$$

$$\text{For } \text{Pr} > 1: u_{max} = n_2 \frac{\nu}{H}\left(\frac{Ra^{\frac{1}{2}}}{Pr}\right) \rightarrow \nu = \frac{u_{max}}{n_2}\left(\frac{Pr}{Ra^{1/2}}\right) H \tag{22}$$

By substituting $u_{max} \leq 0.1$ and equations 5 and 6 into equations 21 and 22, we obtain the best relaxation times.

**Table 2**
The best relaxation times for natural convection in different Prandtel ranges.

| Prandtel number | $\tau_v$ | $\tau_c$ |
|---|---|---|
| Pr < 1 | $\left(\frac{0.1}{n_1}\right)\left(\frac{1}{c_s^2\,\Delta t}\right)\left(\frac{Pr}{Ra}\right)^{\frac{1}{2}} + 0.5$ | $\left(\frac{0.1}{n_1}\right)\left(\frac{1}{c_s^2\,\Delta t}\right)\left(\frac{1}{RaPr}\right)^{\frac{1}{2}} + 0.5$ |
| Pr > 1 | $\left(\frac{0.1}{n_2}\right)\left(\frac{1}{c_s^2\Delta t}\right)\left(\frac{Pr}{Ra^{\frac{1}{2}}}\right) + 0.5$ | $\left(\frac{0.1}{n_2}\right)\left(\frac{1}{c_s^2\Delta t}\right)\left(\frac{1}{Ra^{\frac{1}{2}}}\right) + 0.5$ |

It can be seen from this table, that while we have high lattice grids a larger relaxation time can be obtained. Therefore, better stability is reached. Moreover, the presence of $n_1$and $n_2$ in the denominators of the above equations, as they are less than unity, gives us a better dominance over the range in which we can choose the relaxation time from.

## Problem definition

In this part, the lattice Boltzmann simulation of a convective flow and thermal fields in a 3-D differentially heated in a cubical cavity without/with two and three rectangular parallelepiped vertical fins is presented to illustrate the applicability of this method.

The boundary conditions for the mentioned problem are shown in Fig.1a, that shows a cubical enclosure of side Hand all surfaces are perfectly isolated and adiabatic except two opposite surfaces specified by red and blue colors. The mentioned surfaces are isothermal and maintained at different temperatures $T_h$ and $T_c$($T_h > T_c$) respectively.

As a second geometry, Figure 1b shows a cubical enclosure of side H containing two and three rectangular parallelepiped vertical fins attached to the hot wall with the length, width, and height of $L_f = 0.1H$, $w_f = 0.03H$, and $h_f = H$, respectively.

In the state that cubical enclosure containing two vertical fins, distance between two fins is $S = 0.4H$ and In the state that cubical enclosure containing three vertical fins, distance between each fins is $S = 0.2H$. The flow is considered incompressible.

Boussinesq approximation has been used to express the momentum equation, in which all fluid properties are assumed constant except the density whose varying with the temperature.

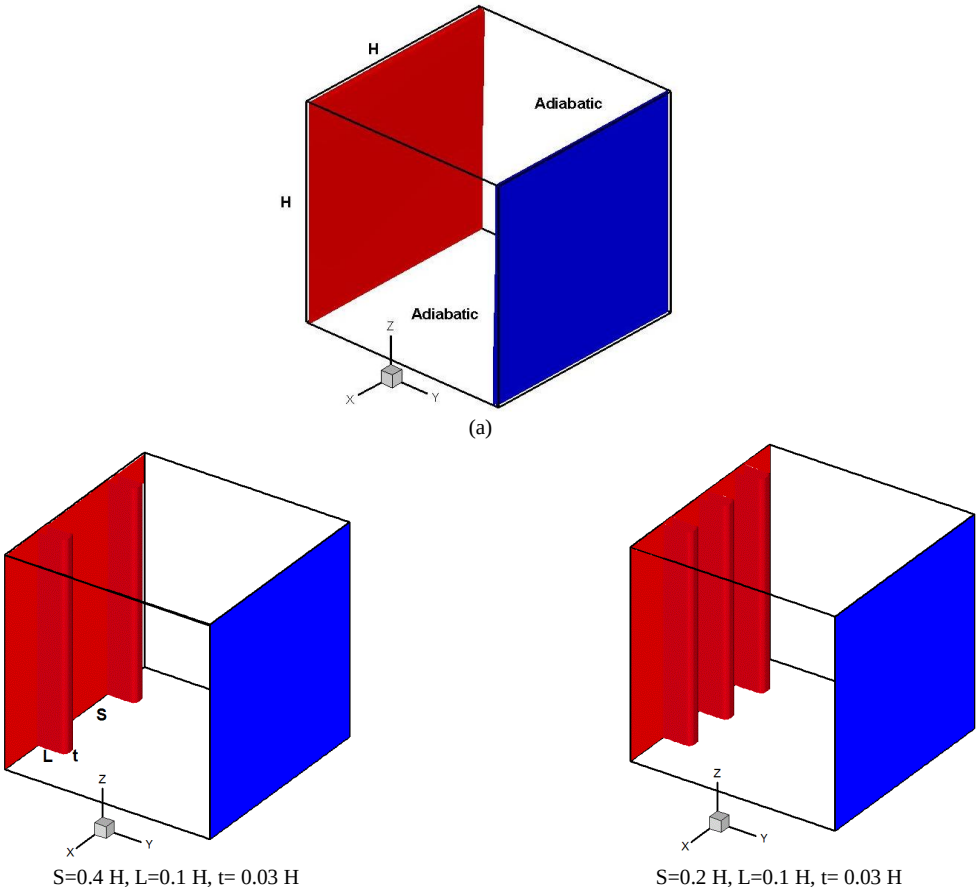



**Fig.1.** The schematic of the natural convection in the differentially heated cubical cavity (a) without the fin, and (b) with two/three vertical fin

## Parameters specification

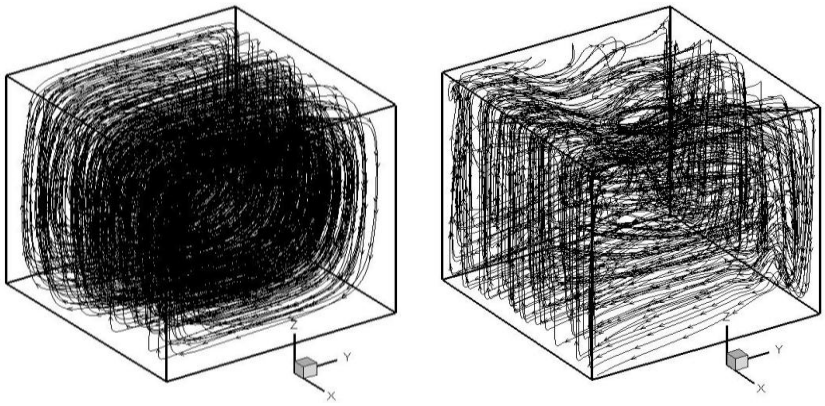
As an assessment way of natural convection problems, Nusselt number (Nu) is defined here by the temperature gradient as walls maintained at a constant temperature:

$$Nu_y = -\frac{H}{\Delta T}\left(\frac{\partial T}{\partial y}\right)_{wall} \tag{23}$$

$$Nu_m = \frac{1}{H}\int_0^H Nu_y dy \tag{24}$$

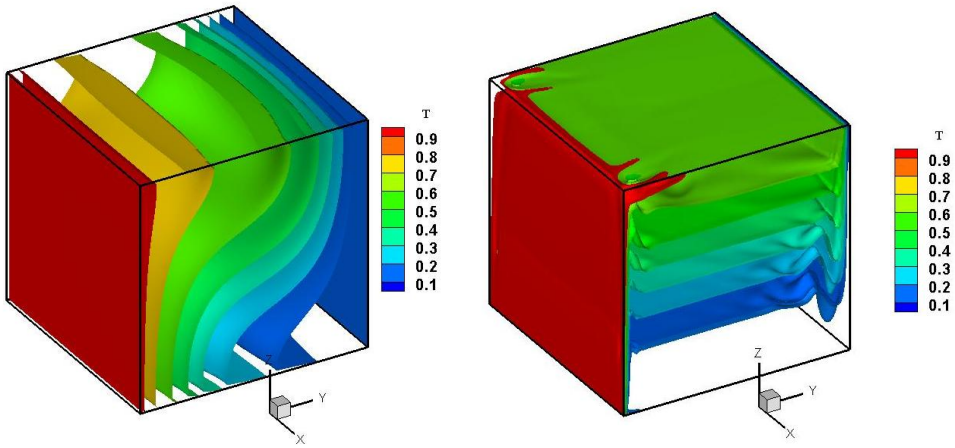
## Validation code for Lattice Boltzmann method

3D schematics of streamlines and isotherms for the benchmark problem are shown in Figure 2 and 3.




(a) (b)

**Fig. 2.** 3D schematics of streamlines for the benchmark problem at (a) Ra=$10^4$ (b) Ra=$10^8$




(a) (b)

**Fig. 3.** 3D schematics of isotherms for the benchmark problem at (a) Ra=$10^{4,}$ (b) Ra=$10^{8}$

When the Rayleigh number is equal to $10^4$ , isotherms are first Perpendicular to the thermal surface and with increasing temperature isotherms are Perpendicular to the adiabatic surface.

Lattice grids that use for this simulation are 80×80×80 for $10^3 \leq Ra \leq 10^7$ and 100×100×100 for Ra $= 10^8$.

Table 3, presents a full comparison of different flow and heat transfer characteristics.

It can be observed that our simulation results are in good agreement with Rui and Wenwen Liu [21].

Since, we obtained better results, with a 100×100×100 lattice grid, in comparison with Rui and Wenwen Liu, who solved the problem with a 256×256 lattice grid and the multiple-relaxation-time Lattice Boltzmann Method.

**Table 3**
Comparison of the results with previous work on the symmetry plane of x=0.5.

| **Ra** | **$10^3$** | **$10^4$** | **$10^5$** | **$10^6$** | **$10^7$** | **$10^8$** |
|---|---|---|---|---|---|---|
| **Grid used** | 80×80×80 | 80×80×80 | 80×80×80 | 80×80×80 | 80×80×80 | 100×100×100 |
| **$Nu_m$ in present study** | 1.113 | 2.231 | 4.520 | 8.845 | 16.499 | 29.590 |
| **$Nu_m$ in Ref. [21]** | 1.108 | 2.252 | 4.596 | 8.822 | 16.424 | 29.094 |

## RESULTS AND DISCUSSION

The streamlines and isothermal lines are displayed in Figures 4-9.

It is shown in Figures 4 that streamlines in a cubical cavity with two vertical fins and also in Figures 5, three vertical fins.

When the Rayleigh number increase, streamlines in a cubical cavity with three vertical fins are growth more than streamlines in a cubical cavity with two vertical fins.

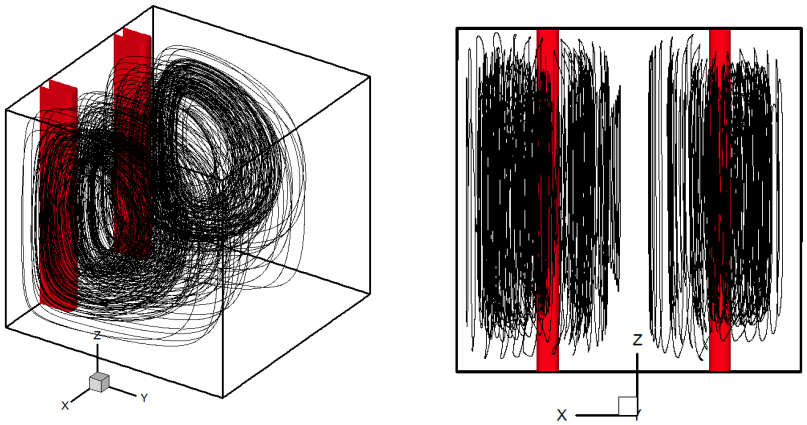
At low Rayleigh number (Ra), a central vortex appears as the typical feature of the flow.

With the increment of Rayleigh number, a n elliptic shape tends to be formed. With Comparison between Figures 4 and 5 We find out that streamlines in a cubical cavity with three vertical fins is compressed than streamlines in a cubical cavity with two vertical fins.

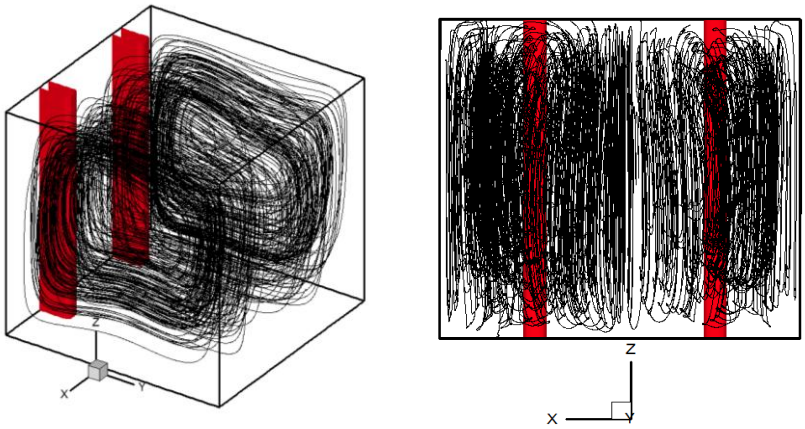
It is shown in Figures 6 those isothermal lines in cubical cavity with two vertical fins and also in Figures 7, three vertical fins.

In low Rayleigh number (Ra), isothermal lines are almost parallel and in line with vertical fins. With the increment of Rayleigh number, isothermal lines are almost perpendicular with vertical fins.

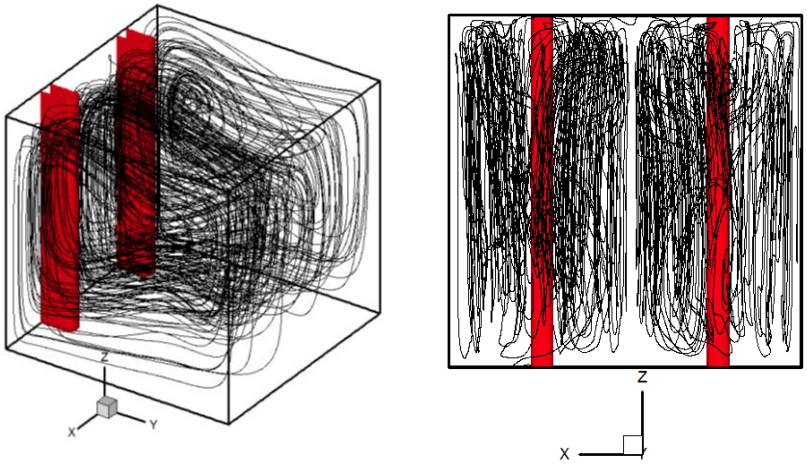
In cubical cavity with two vertical fins when the Rayleigh number is increase, isothermal lines are first Perpendicular to the thermal surface and with increasing temperature isothermal lines are Perpendicular to the adiabatic surface that this situation is clear in cubical cavity with three vertical fins.




Ra=$10^4$




Ra=$10^5$




Ra=$10^6$

**Fig. 4.** 3D schematics for streamlines in a cubical cavity with two vertical fins$(10^4 \leq Ra \leq 10^6)$

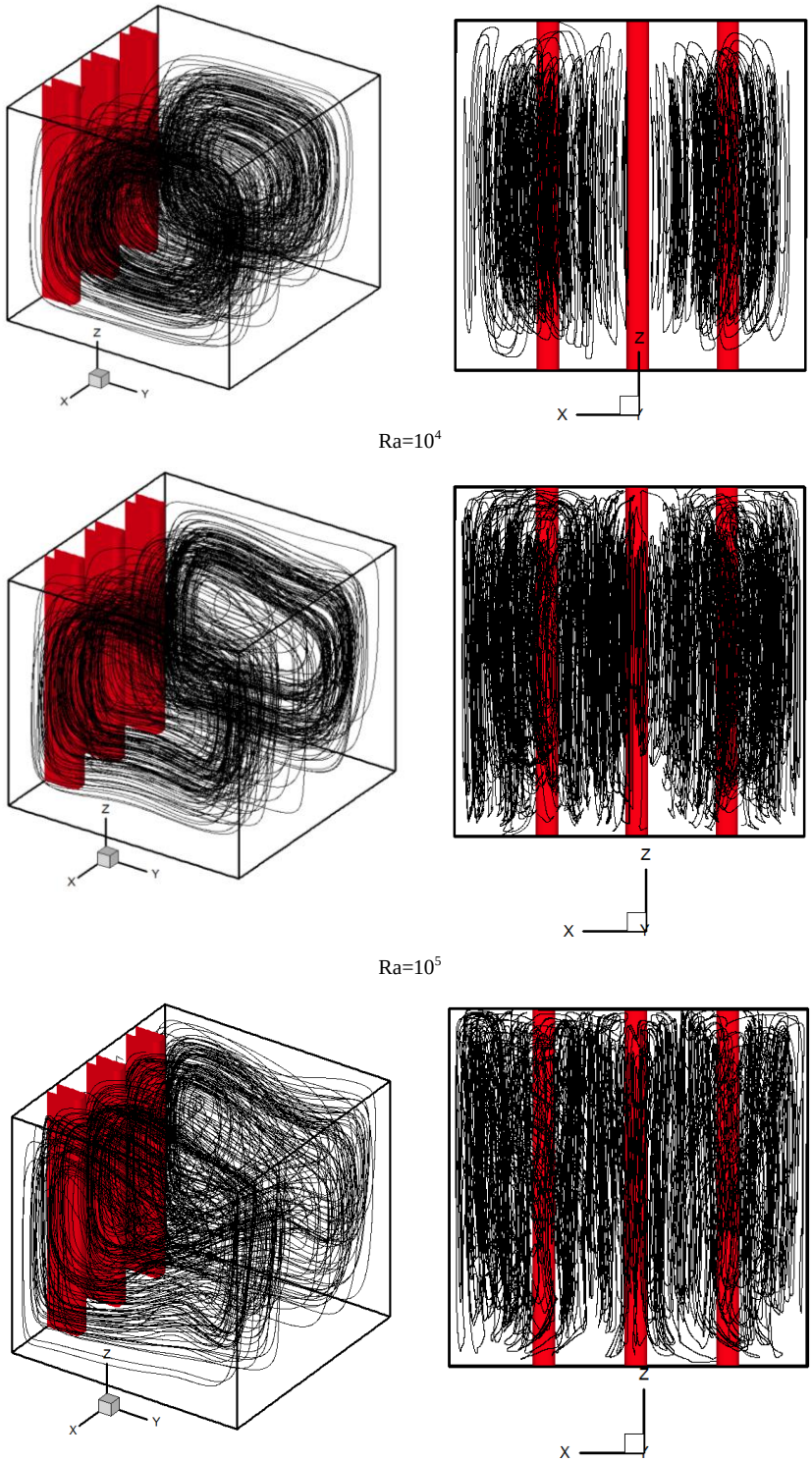



**Fig. 5.** 3D schematics for streamlines in a cubical cavity with three vertical fin$(10^4 \leq Ra \leq 10^6)$

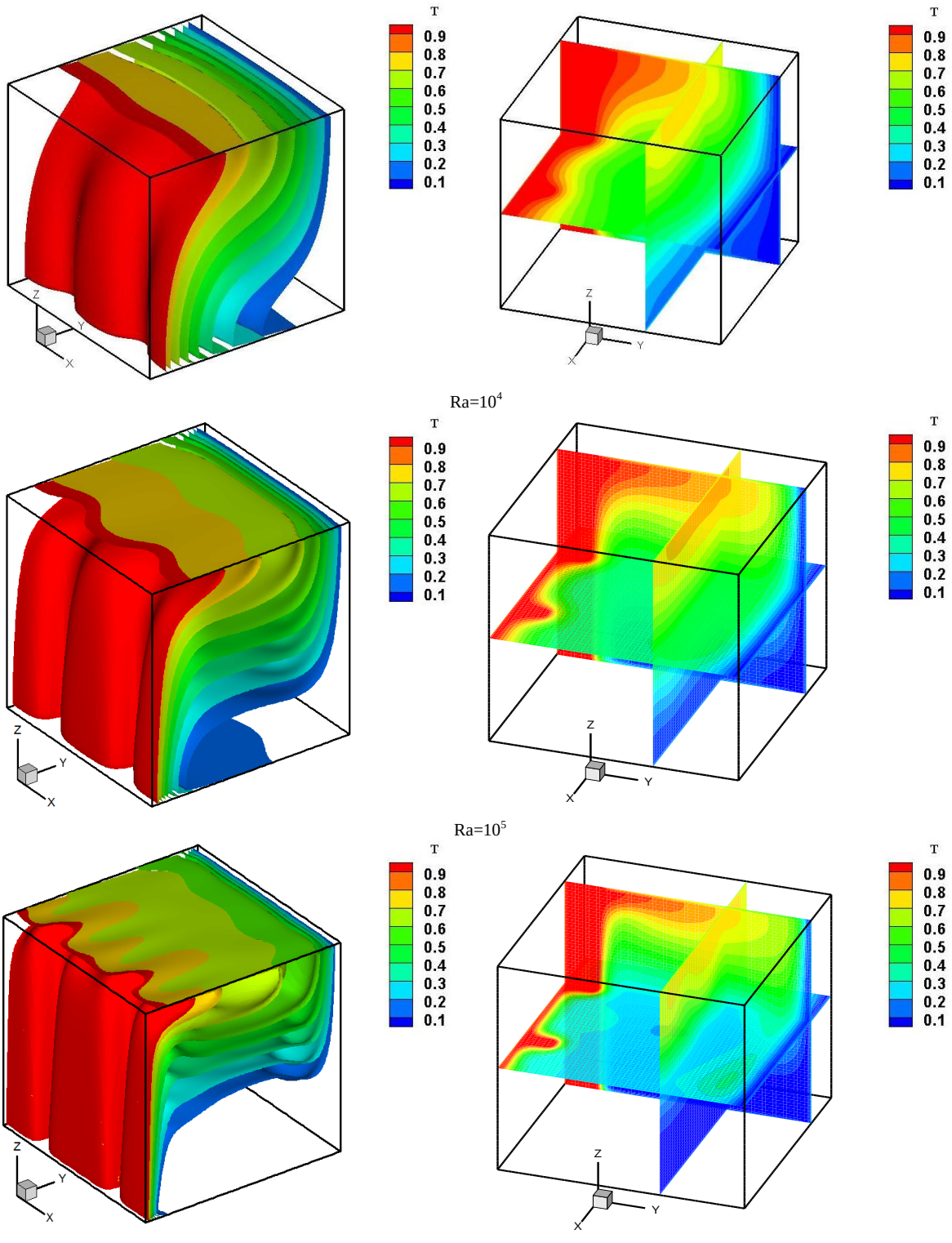



**Fig. 6.** 3D schematics for isothermal lines in a cubical cavity with two vertical fins($10^4 \leq Ra \leq 10^6$)

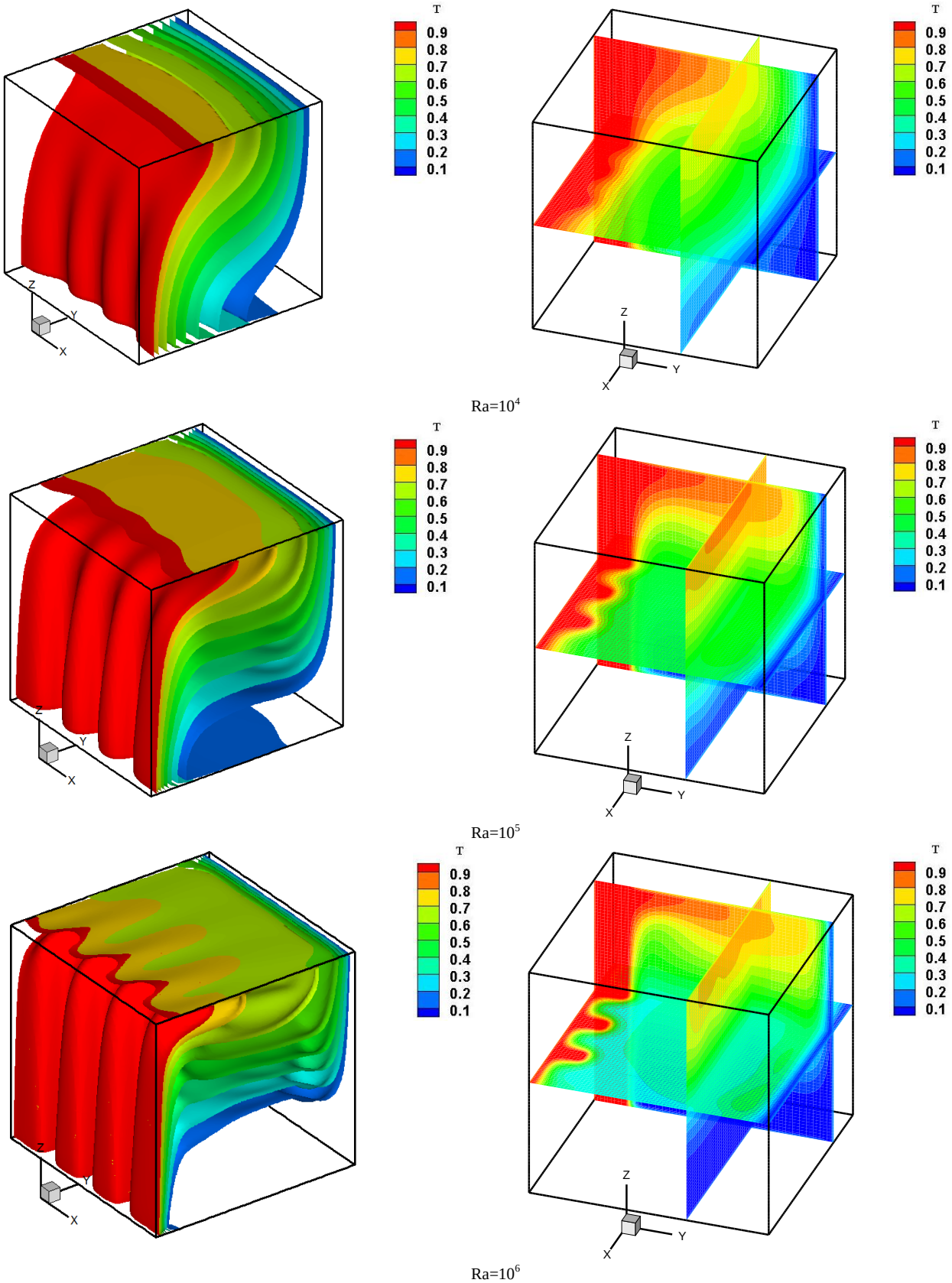



**Fig. 7.** 3D schematics for isothermal lines in a cubical cavity with three vertical fins($10^4 \leq Ra \leq 10^6$)

Figure 8 and 9 show the isothermal lines and temperature profile between fins in a cubical cavity at Ra =$10^4$-$10^6$. Temperature profiles are displayed in different height of the fins. By attention to the Figures we can find out with the increased height of the fins, Temperature profile become smooth. With the growth of the Rayleigh number (Ra) up to $10^6$, the temperature gradient is increased.

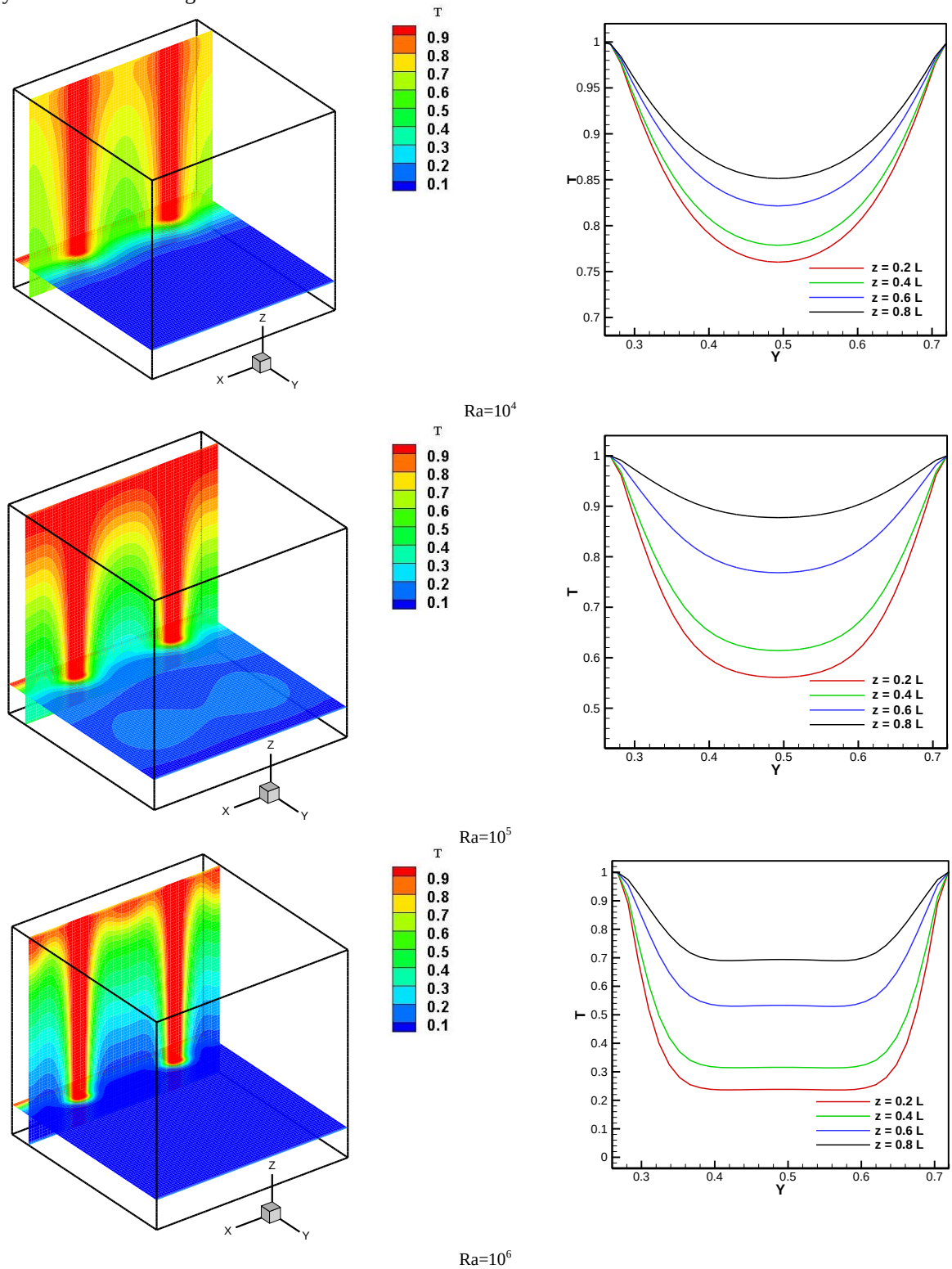
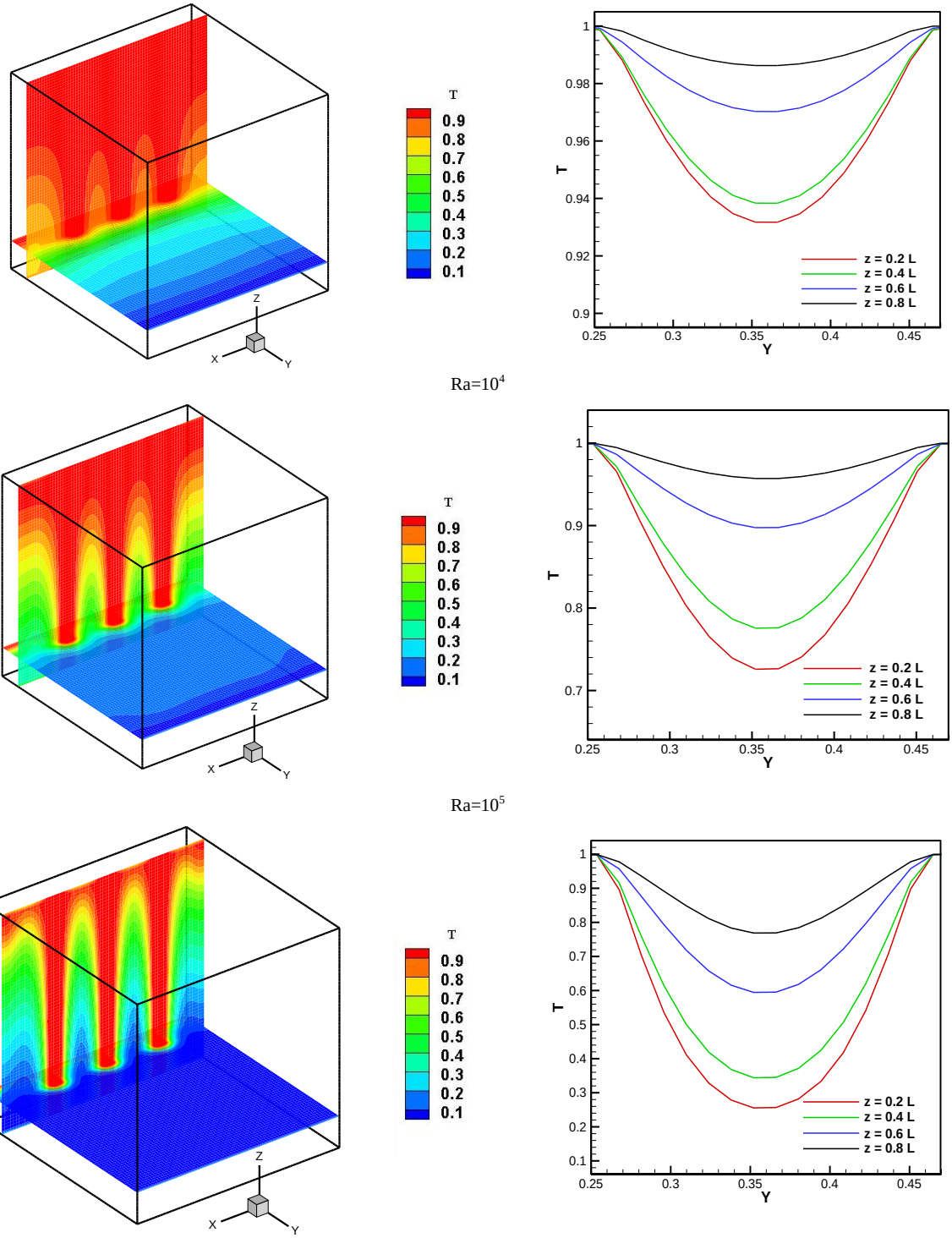



**Fig. 8.** 2D schematics for isothermal lines in a cubical cavity with two vertical fins $(10^4 \leq Ra \leq 10^6)$

Optimum conditions happen when the edges of the thermal boundary layer reach together between each of two fins (Ra =$10^6$ with three fins). That's mean not so much distance of each other (Ra =$10^6$ with two fins) is not suitable, because in this case, our surface area will not have the maximum value and nor when the fins are too close together (Ra =$10^4$ with three fins), because in this position, we will have very low Nusselt number.




Ra=$10^4$

Ra=$10^5$

Ra=$10^6$

**Fig. 9.** 2D schematics for isothermal lines in a cubical cavity with three vertical fins ($10^4 \leq Ra \leq 10^6$)

Figure 10a shows that with an increase in vertical fins the Nusselt number decreases in cubical cavity. The Nusselt Number versus in terms of Rayleigh number are depicted in Figure 10b for different nanofluids ($CuO$,$Al_2O_3$) and volume fractions ($\phi = 0.01, \phi = 0.03$). As described above, this figure also confirms that increasing the Rayleigh number can enhance to increase the Nusselt number in the natural convection heat transfer.

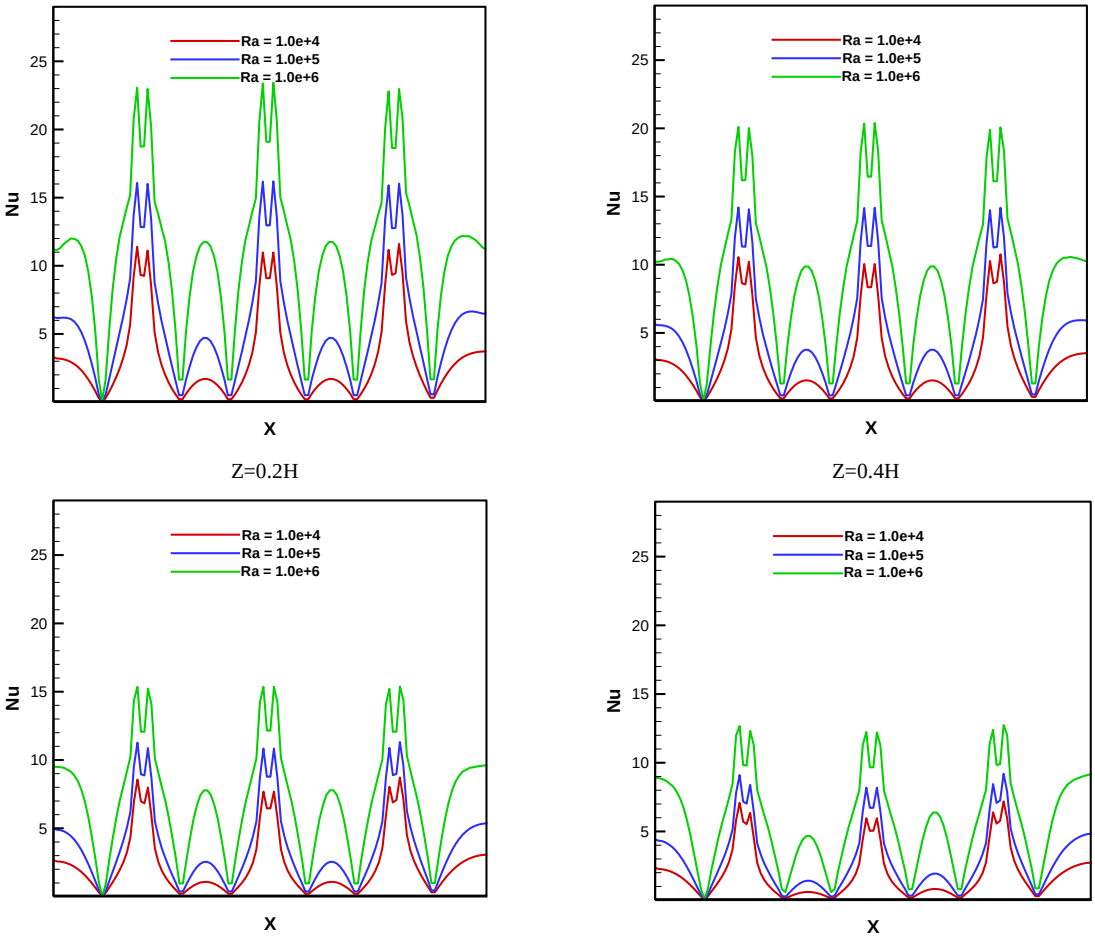



**Fig. 10.** Local Nusselt number at different level for surfaces with three fins

Figures 11 show that comparing between the local Nusselt number at different levels for surfaces with two and three fins. Totally increases in local Nusselt numbers are observable by increasing Rayleigh number. Also, these figures express that when the distance between each of two fins increases, so the maximum of local Nusselt number decreases and the Nusselt profiles become more smooth.

Table 4, 5 and 6 presents Heat transfer characteristics in Cubical cavity in Ra =$10^4$, $10^5$ and $10^6$.

**Table 4**
Heat transfer characteristics in Cubical cavity in Ra =$10^4$.

| | **Three fins** | **Two fins** | **Without fin** |
|---|---|---|---|
| **Nusselt number (Nu)** | 0.61 | 1.70 | 2.29 |
| $A_{DL} = \frac{A}{A_{wf}}$ | 1.85 | 1.57 | 1.00 |
| $q_{DL} = \frac{q_f}{q_{without\ fin}}$ | 0.49 | 1.16 | 1.00 |

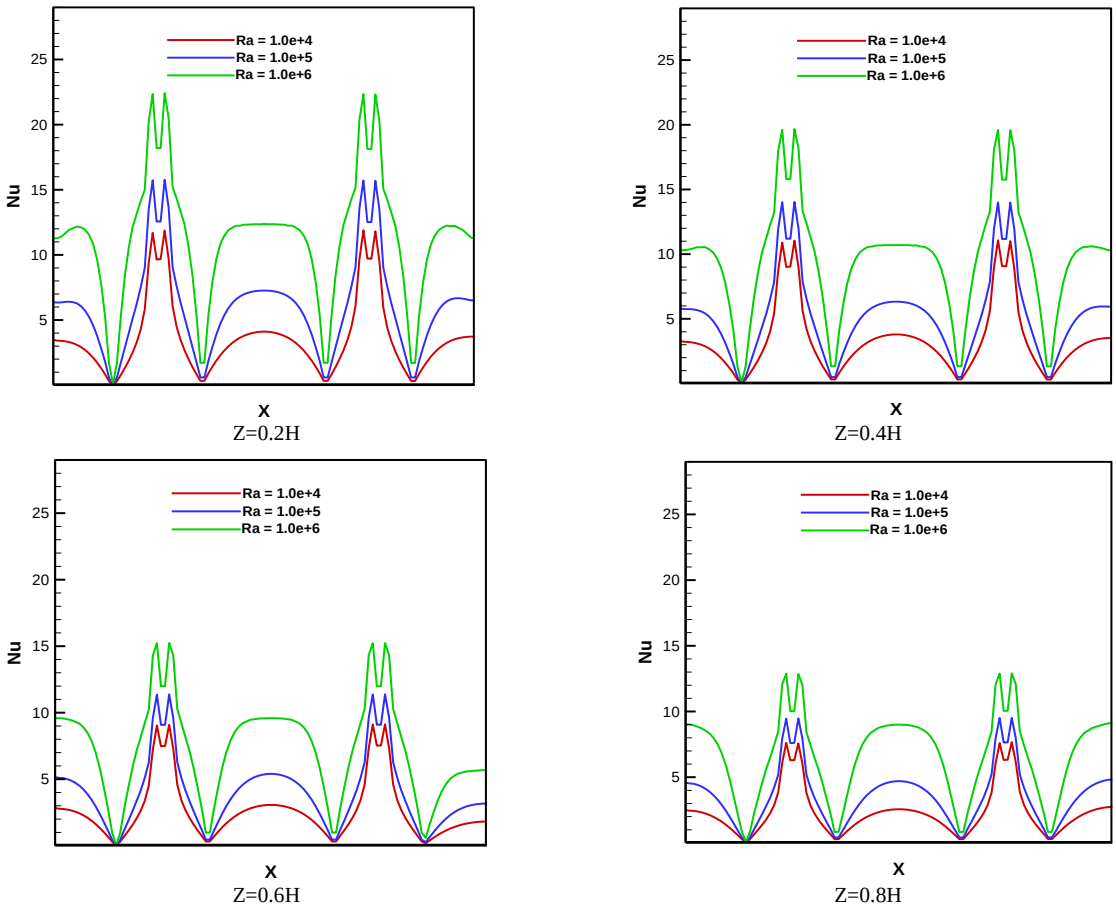



**Fig. 11.** Local Nusselt number at different level for surfaces with two fins

$A_{DL}$ is the ratio of the total surface of hot wall of the cubical cavity (sum of the base surface and fin surface) rather than the base surface without fin.

By Looking at the Table 4, we find out that in Ra=$10^4$, the Nusselt number (Nu) decreases to the rate 25.8% for two fins and 73.4% for three fins by $A_{DL}$ increases. Table 5, shows that when the Rayleigh number (Ra) increases, these decreasing procedures happen to the rate of 11.6 % for two fins and 55.8 % for three fins.

Respectively, in Table 6this phenomenon occurs with a rate of 9.4 % for two fins and 16.5 % for three fins.

**Table 5**
Heat transfer characteristics in Cubical cavity in Ra =$10^5$.

| | **Three fins** | **Two fins** | **Without fin** |
|---|---|---|---|
| **Nusselt number (Nu)** | 2.02 | 4.04 | 4.57 |
| $\boldsymbol{A_{DL} = \frac{A}{A_{wf}}}$ | 1.85 | 1.57 | 1.00 |
| $\boldsymbol{q_{DL} = \frac{q_f}{q_{without\ fin}}}$ | 0.82 | 1.38 | 1.00 |

By accurate observation of $q_{DL}$, rate of Heat transfer with fin per Heat transfer rate without fin in Cubical cavity due to the Tables, we find out that in Ra =$10^4$by increasing $A_{DL}$, the $q_{DL}$increases in the rate16 % for two fins and decreases to the rate 51 % for three fins.

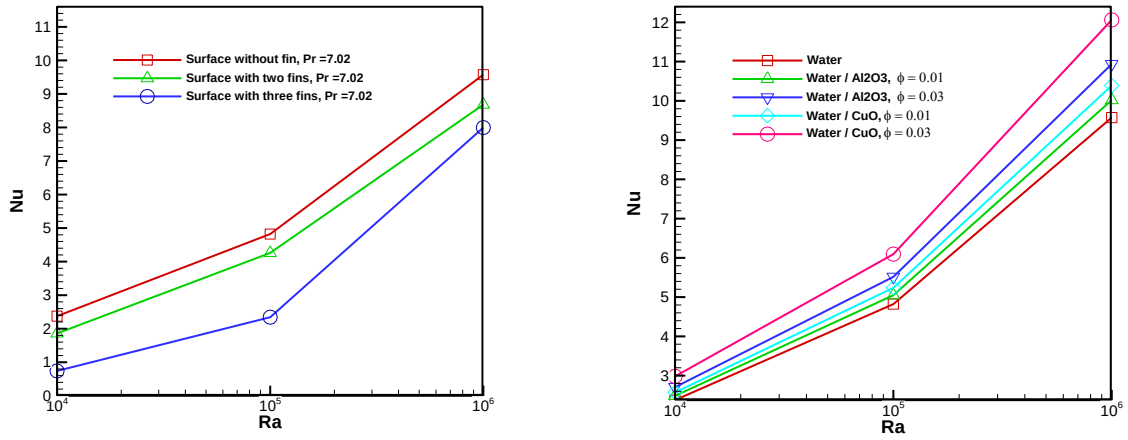
Table 5 shows that the $q_{DL}$ increases in the rate 38 % for two fins and decreases to the rate18 % for three fins.

Respectively, in Table 6 at Ra =$10^6$, by increasing $A_{DL}$, the $q_{DL}$ increases to the rate 42 % for two fins and 60 % for three fins.

**Table 6**
Heat transfer characteristics in Cubical cavity in Ra =$10^6$.

| | **Three fins** | **Two fins** | **Without fin** |
|---|---|---|---|
| **Nusselt number (Nu)** | 7.77 | 8.43 | 9.30 |
| $A_{DL} = \frac{A}{A_{wf}}$ | 1.85 | 1.57 | 1.00 |
| $q_{DL} = \frac{q_f}{q_{without\ fin}}$ | 1.60 | 1.42 | 1.00 |

Figures 12 is plotted for Comparison Changes the Nusselt number in a cubical cavity with the effect of vertical fins and nanofluid with water as the base fluid (Pr=7.02).




(a) (b)

**Fig. 12.** Changes the Nusselt number in cubical cavity with the effect of (a) vertical fins and (b) nanofluid

Finally, according to Table 7, the maximum Nusselt number reveals for Cuo/water nanofluid at Ra=$10^6$ and $\phi = 0.03$ that is equal with 12.062.This results show that by using nanofluid, we can earn 26 % increment in heat transfer rate.

**Table 7**
Changes the Nusselt number with the effect of vertical fins and nanofluid ($10^4 \leq Ra \leq 10^6$).

| **Ra** | **$10^4$** | **$10^5$** | **$10^6$** |
|---|---|---|---|
| **Heat transfer in a cubical cavity filled with water (Pr =7.02)** | Nusselt number (Nu) | | |
| **surface with three vertical fins** | 0.741 | 2.343 | 7.997 |
| **surface with two vertical fins** | 1.859 | 4.259 | 8.681 |
| **surface without vertical fins** | 2.375 | 4.822 | 9.574 |
| **Heat transfer in a cubical cavity filled with nanofluid** | Nusselt number (Nu) | | |
| **surface without fin, water/ $Al_2O_3$, $\phi = 0.01$,** | 2.484 | 5.048 | 10.020 |
| **surface without fin, water/ CuO, $\phi = 0.01$** | 2.707 | 5.517 | 10.938 |
| **surface without fin, water/ $Al_2O_3$, $\phi = 0.03$** | 2.573 | 5.237 | 10.389 |
| **surface without fin, water/ CuO, $\phi = 0.03$** | 2.981 | 6.095 | 12.062 |

## CONCLUSION

This paper presents a comprehensive numerical analysis of three-dimensional fluid flow and heat transfer in a cubical cavity with vertical fins by solving the temperature and flow field with LBGK D3Q19 model. We observed in Ra =$10^6$ by increasing $A_{DL}$, the $q_{DL}$ increases to the rate 42

% for two fins and 60 % for three fins. Also The $q_{DL}$ in Ra = $10^6$ for cubical cavity with three fins is more than all. Moreover, the optimum number of fins is a function Rayleigh number and dimension of the cavity, for Ra=$10^4$ and $10^6$ the optimum arrangement is two and three fins, respectively. After that increasing in the number of vertical fins, which leads to increase in the warm wall area, consequently it can enhance to increase the Nusselt number in cubical cavity. Finally, by using nanofluid, we can earn 26 % increment in heat transfer rate.

## REFERENCES


[1] McNamara G R, Zanetti G. Three dimensional lattice boltzmann simulation of steady and transient finned natural convection problems with evaluation of different forcing and conjugate heat transfer schemes. Computers and Mathematics with Applications. 2017 Sep 15;74(6):1362-1378.

[2] McNamara G R, Zanetti G. Use of the soltzmann equation to simulate lattice-gas automata. Physical Review Letters. 1988 Nov 14;61(20):2332-2335.

[3] Gladrow D W, Lattice-Gas Cellular Automata and Lattice Boltzmann Models. Springer. 2000;1725:X 314.

[4] Kuznik F, Obrecht C, Rusaouen G, Roux J J. LBM based flow simulation using GPU computing processor. Computers and Mathematics with Applications. 2010 Apr 24;59(7):2380-2392.

[5] Zou Q, He X. On pressure and velocity boundary conditions for the lattice Boltzmann BGK model. American Institute of Physics. 1997 Jun 4;9(6): 1591-1598.Shah RK, London AL. Laminar Flow Forced Convection in Ducts. Academic Press, New York. 1978.

[6] Vajjha R, Das D, Namburu P. Numerical study of fluid dynamic and heat transfer performance of $Al_2O_3$ and CuO nanofluids in the flat tubes of a radiator. Int. J. Heat Fluid Flow. 2010; 31: 613–21.

[7] Safikhani H, Abbassi A. Effects of tube flattening on the fluid dynamic and heat transfer performance of nanofluid flow. Adv. Powder Technolog. 2014; 25(3):1132-41.

[8] Safikhani H, Abbassi A, Khalkhali A, Kalteh M. Multi-objective optimization of nanofluid flow in flat tubes using CFD, Artificial Neural Networks and genetic algorithms. Adv. Powder Technolog. 2014; 25(5): 1608-17.

[9] Saltelli A, Sobol IM. About the use of rank transformation in sensitivity analysis of model output. Reliability Engineering & System Safety.1995 ; 50(3) : 225-39

[10] Saltelli A, Chan K, Scott E. Sensitivity analysis Wiley series in probability and statistics. Willey, New York. 2000

[11] Korayem M, Rastegar Z, Taheri M. Sensitivity analysis of nano-contact mechanics models in manipulation of biological cell. Nanoscience and Nanotechnology. 2012 ; 2(3):49-56.

[12] Quiben J, Cheng L, Da Silva J, Thome J. Flow Boiling in horizontal flattened tubes: Part I – Two-phase frictional pressure drop results and model. Int. J. Heat Mass Transf. 2009; 52(15-16): 3645-53.

[13] Kim D, Kwon Y, Cho Y, Li C, Cheong S, Hwang Y, Lee J, Hong D,Moon S. Convective heat transfer characteristics of nanofluids under laminar and turbulent flow conditions. Current Applied Physics. 2009; 9(2): 119-23.

[14] Ebrahimnia-Bajestan E, Niazmand H, Duangthongsuk W, Wongwises S. Numerical investigation of effectiv parameters in convective heat transfer of nanofluids flowing under a laminar flow regime. Int. J. Heat Mass Transf. 2010; 54 (19-20): 4376-88.

[15] Tong C. Self-validated variance-based methods for sensitivity analysis of model outputs. Reliability Engineering & System Safety. 2010; 95 (3): 301-9.

[16] Nossent J, Elsen P, Bauwens W. Sobol'sensitivity analysis of a complex environmental model. Environmental Modelling & Software. 2011; 26(12): 1515-25.

[17] Sobol IM. Sensitivity estimates for nonlinear mathematical models. Mathematical Modeling and Computational Experiments.199; 14; 407-14.

[18] Cukier R, Levine H, Shuler K. Nonlinear sensitivity analysis of multiparameter model systems. Journal of computational physics.1978; 26(1): 1-42.

[19] Saltelli A, Tarantola S, Chan KS. A quantitative model-independent method for global sensitivity analysis of model output. Technometrics. 1999; 41, 39-56.

[20] Homma T, Saltelli A. Importance measures in global sensitivity analysis of nonlinear models. Reliability Engineering & System Safety.1996; 52:1-17.